

Selective Metal Cation Capture by Soft Anionic Metal–Organic Frameworks via Drastic Single-Crystal-to-Single-Crystal Transformations

Jian Tian,[†] Laxmikant V. Saraf,[†] Birgit Schwenzer,[†] Stephanie M. Taylor,[‡] Euan K. Brechin,[‡] Jun Liu,[†] Scott J. Dalgarno,^{*,§} and Praveen K. Thallapally^{*,†}

[†]Pacific Northwest National Laboratory, Richland, Washington 99352, United States

[‡]EaStCHEM School of Chemistry, University of Edinburgh, Edinburgh EH9 3JJ, U.K.

[§]Institute of Chemical Sciences, Heriot-Watt University, Riccarton, Edinburgh EH14 4AS, U.K.

Supporting Information

ABSTRACT: Flexible anionic metal–organic frameworks (MOFs) are transformed into neutral heterobimetallic systems via single-crystal-to-single-crystal processes invoked by cation insertion. These transformations are directed by cooperative bond breakage and formation, resulting in expansion or contraction of the 3D framework by up to 33% due to the flexible nature of the organic linker. These MOFs displays highly selective uptake of divalent transition-metal cations (e.g., Co^{2+} and Ni^{2+}) over alkali-metal cations (Li^+ and Na^+).

Metal–organic frameworks (MOFs) have been widely investigated because of their potential applications in areas such as gas storage/separation,^{1,2} ion exchange,³ magnetism,⁴ catalysis,⁵ and nonlinear optics.⁶ Flexible MOFs have received particular recent attention because they can exhibit structural transformations upon single-crystal-to-single-crystal (SC–SC) processes triggered by external stimuli,^{7,8} a feature that can be accompanied by fascinating changes in host–guest behavior,^{9,10} magnetism,¹¹ and photochemical reactivity,¹² for example. Such transformations are generally accompanied (or generated) by the removal/addition of guest molecules¹³ or exchange of coordinated metal ions or counterions,^{14,15} processes in which the framework integrity is often retained. A seminal example of flexible MOF formation is MIL-53 as reported by Férey and co-workers.¹⁶ The cell volume in said system varies by $\sim 40\%$ between large-pore and narrow-pore forms, with respective expansion/contraction of the frameworks during adsorption/desorption of suitable guest molecules. In general, SC–SC processes involving the robust rearrangement of framework structures are comparatively rare because single crystals usually fail to maintain their crystallinity upon transformation. Herein we report soft anionic MOFs, constructed from the flexible organic linker tetrakis[4-(carboxyphenyl)oxamethyl]methane acid (H_4L) (Figure 1A), that act as transition metal (TM) cation receptors via ligand-directing SC–SC structural rearrangement (Figure 1B,C). These transformations involve incorporation of TM^{2+} cations into the anionic networks to afford neutral and heterobimetallic systems. To the best of our knowledge, this represents the first documented report of capture of metal ions by soft anionic

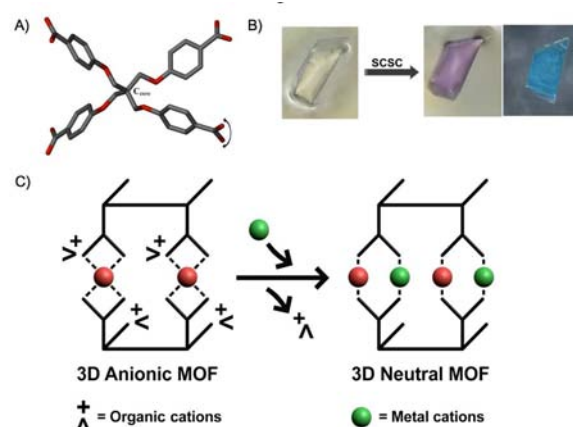


Figure 1. (A) Structure of the semirigid carboxylate linker tetrakis[4-(carboxyphenyl)oxamethyl]methane acid (H_4L) (C, gray; O, red). Flexibility arises from twisting of the benzoate moieties around the central quaternary carbon atom (denoted as C_{core}) through ether links. (B) Photographs of crystals before and after TM^{2+} capture. (C) Scheme showing the incorporation of TM^{2+} cations into the anionic networks to afford neutral and heterobimetallic systems via ligand-directing SC–SC structural rearrangement.

MOFs in the solid state, the transformations of which involve cooperative bond breaking and formation rather than the more frequently encountered counterion-exchange mechanism.^{3,14,15b}

Interest in the coordination chemistry of H_4L has been driven by both its flexibility and its varied mode of coordination with TM ions.¹⁷ The reaction of H_4L with Zn^{2+} under different conditions affords seven isomers based on different Zn clusters that act as secondary building units (SBUs).¹⁸ Diverse ligand geometries such as tetrahedral, irregular, or near-flattened are observed in these solids, and this flexibility arises from twisting of the benzoate moieties around the central quaternary carbon atom (denoted as C_{core} in Figure 1A) through ether links. With this in mind, we sought to explore the potential for constructing stimuli-responsive flexible MOFs from H_4L . A series of isostructural anionic MOFs with the general formula $[\text{M}_3(\text{L})_2]^{2-} \cdot 2[\text{NH}_2(\text{CH}_3)_2]^+ \cdot 8\text{DMA}$ ($\text{M} = \text{Co}, \text{Mn}, \text{Cd}$; DMA

Received: March 30, 2012

Published: May 25, 2012

= *N,N*-dimethylacetamide) were recently reported by Cao and co-workers.¹⁹ These MOFs crystallize in the triclinic space group $P\bar{1}$, and the asymmetric unit comprises one L^{4-} ligand, two crystallographically independent TM^{2+} ions, and a $[NH_2(CH_3)_2]^+$ counterion generated in situ under solvothermal conditions. One of the TM^{2+} ions is in a general position, while the other resides on an inversion center with 50% site occupancy. In our hands, two MOFs with the general anionic framework formula $[Mn_3(L)_2]^{2-}$ (**1**) were obtained under solvothermal conditions from differing ratios of *N,N*-dimethylformamide (DMF) and water: $[Mn_3(L)_2]^{2-} \cdot 2 \cdot [NH_2(CH_3)_2]^+ \cdot 9DMF$ (**1a**) and $[Mn_3(L)_2]^{2-} \cdot 2 \cdot [H_3O]^+ \cdot 12DMF$ (**1b**) [for experimental details, see the Supporting Information (SI)]. Single-crystal X-ray diffraction (SCXRD) studies revealed that both structures display the same connectivity between the Mn_3 SBUs and L^{4-} linkers, resulting in anionic 3D frameworks with the same topology but disparate counterions (Figure S1 in the SI). Although this is the case, different conformations of L^{4-} in the solids results in varied dimensionality in **1a** and **1b**; the unit cell volume of **1a** ($V = 2671 \text{ \AA}^3$) is 14% smaller than that of **1b** ($V = 3052 \text{ \AA}^3$). Comparison of the conformations of L^{4-} in **1a** and **1b** clearly shows that along the *a* axis, two of the four arms of L^{4-} are more splayed in **1b** than in **1a**, causing the *a* axis of **1b** to be 1.7 Å longer (Figure S2). Thus, the anionic framework of **1b** can be regarded as an “expanded” form of **1a**. The flexibility of L^{4-} within these anionic MOFs prompted us to investigate the possibility of exchanging the Mn^{2+} or $NH_2(CH_3)_2^+/H_3O^+$ ions with other TM^{2+} ions such as Co^{2+} , Cu^{2+} , and Ni^{2+} .

A colorless single crystal of **1a** was fixed to the top of a glass fiber and immersed in a 0.2 M DMF solution of cobalt(II) nitrate. The crystal did not dissolve but turned to light-purple color within a few hours, indicating penetration of Co^{2+} into the framework. After 24 h, a deep-purple crystal of **2** was obtained and analyzed crystallographically. Surprisingly, the crystal structure of **2** is significantly different from that of **1a**, despite the fact that they have the same space group and similar unit cell parameters. The asymmetric unit of **2** comprises one L^{4-} linker, one aqua ligand, and three crystallographically independent Mn^{2+}/Co^{2+} ions; two of these reside on inversion centers with 50% site occupancy while the third occupies a general position. In comparison with **1a**, the SBU in **2** becomes neutral by uptake of one TM^{2+} (with 50% site occupancy) per asymmetric unit. On the basis of elemental analysis (EA), thermogravimetric analysis (TGA), and energy-dispersive X-ray spectroscopy (EDX) studies, the formula of **2** was found to be $MnCo_3L_2(H_2O)_2 \cdot 12DMF$. This implies that in addition to insertion of additional Co^{2+} into the framework, partial exchange of Mn^{2+} for Co^{2+} also occurs. Such an insertion/exchange process, proceeding via an SC–SC transformation, must therefore involve the cooperative breakage/formation of metal–carboxylate bonds. This is evidenced by the fact that in moving from **1a** to **2**, two of the four carboxylate groups in the L^{4-} ligand change their coordination modes (Figure S3). To provide a better understanding of the mechanism of the SC–SC transformation, we carefully compared the structural features of these two MOFs. Figure 2 shows extended structures of **1a** and **2** along the *b* axis. In **1a**, the Mn_3 SBUs align along the *c* axis and are mutually interconnected by L^{4-} linkers with a short distance (7.0 Å) between two nearest neighboring clusters. Insertion of Co^{2+} ions in the synthesis of **2** results in linkage of discrete Mn_3 clusters in **1a** to afford an infinite MnCo chain with a zigzag arrangement along the *c* axis.

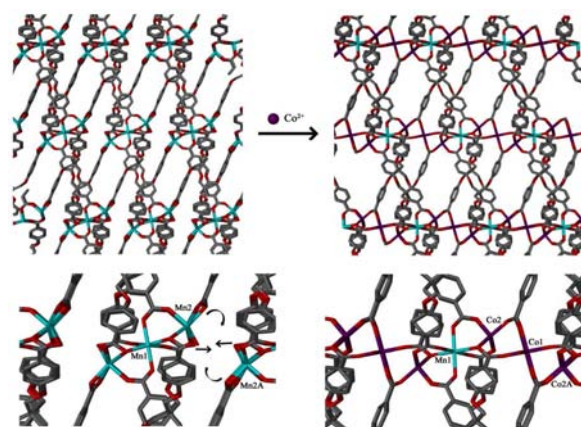


Figure 2. Crystallographic views of (left) **1a** and (right) **2** along the *b* axis (C, gray; O, red; Mn, cyan; Co, purple). The arrows propose how the carboxylate groups coordinated to two nearby terminal Mn^{2+} ions (Mn2 and Mn2A) of the Mn_3 SBUs in **1a** move cooperatively to connect the inserted Co^{2+} (shown as Co1 on the right-hand side).

One octahedral Co^{2+} (Co1 and its symmetry equivalents) resides on an inversion center (between the positions of two neighboring Mn_3 SBUs in **1a**) and is bonded by four carboxylate oxygen atoms from different L^{4-} linkers and two oxygen atoms from aquo ligands. We hypothesize that in order to connect the inserted Co^{2+} (Co1) and meet the constraints of octahedral geometry, the carboxylate groups coordinated to two nearby terminal Mn^{2+} ions (Mn2 and Mn2A) of the Mn_3 SBUs in **1a** must change their coordination modes with a high degree of cooperativity: the chelating carboxylate groups change to bridging mode, the chelating/bridging carboxylate groups change to $\mu_3\text{-}\eta^2\text{:}\eta^1$ -bridging mode, and the bridging carboxylate groups remain the same (Figure 2). This would mean that the terminal octahedral Mn^{2+} ions of the Mn_3 SBUs in **1a** would become four-coordinate with tetrahedral geometry prior to displacement by the Co^{2+} (Co2 and Co2A) ions. This theory is based on the short Co–O bond lengths evident in **2** (four Co–O bonds in the range 1.950–2.043 Å). The variation in the coordination mode of the carboxylate groups is directed by the rotation around C_{core} within the L^{4-} linker, resulting in a slight change in ligand conformation and an expansion of the entire framework by 6.5% in going from **1a** to **2**. Single crystals of **1b** are also transformed into **2** via a similar SC–SC process when treated in an identical fashion, and in this case, the framework contracts by 7.5%, demonstrating that the L^{4-} linker can adjust its conformation to allow for either expansion or contraction of frameworks of **1**.

The insertion of Co^{2+} ions into the anionic framework of **1** indicated that other dications such as Zn^{2+} , Mg^{2+} , Cu^{2+} , and Ni^{2+} may be accommodated, given the degree of ligand versatility observed. Crystals of **1a** were found to capture Cu^{2+} from a DMF solution via a process similar to that for Co^{2+} capture. An intermediate structure of Cu^{2+} -inserted crystals (**1a-Cu**) was successfully solved and found to be isostructural to that of the Co^{2+} -inserted analogue (Figure S4), but these crystals persistently lost their monocrystallinity following completion of the insertion/exchange process over a 24 h period. The insertion of either Mg^{2+} or Zn^{2+} into **1a** resulted in crystal cracking/degradation and loss of single-crystallinity, thus preventing further structural analysis. Notably, crystals of **1a** captured Ni^{2+} ions via an SC–SC process that is significantly different from that for either Co^{2+} or Cu^{2+} . Light-green crystals

of **3** were obtained when **1a** or **1b** was soaked in a 0.2 M DMF solution of nickel(II) nitrate for 24 h. SCXRD analysis revealed that **3** retains the same space group (*PT*) but has a much larger unit cell volume ($V = 3541 \text{ \AA}^3$) than **1a**. The asymmetric unit of **3** comprises one L^4 linker, three and a half aquo ligands, half a ligated DMF, and three crystallographically independent Mn^{2+}/Ni^{2+} ions, implying the insertion of Ni^{2+} into the **1a** framework. EA, TGA, and EDX studies indicated the formula of **3** to be $Mn_{1.3}Ni_{2.7}L_2(H_2O)_7(DMF) \cdot 16DMF$. Comparison of the structural features of **1a** and **3** indicates how the SC–SC transformation proceeds. Figure 3 shows views of **1a** and **3**

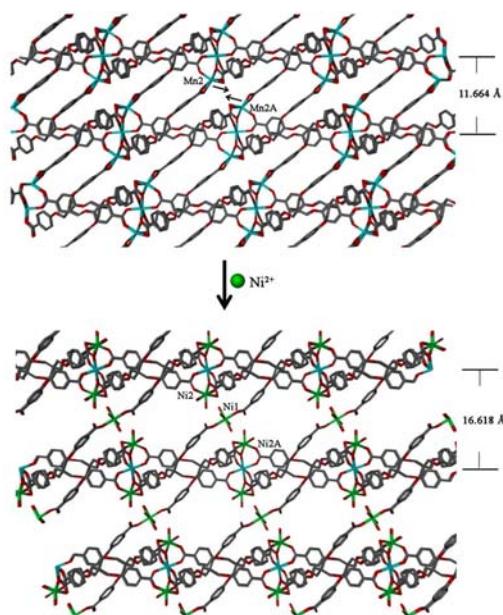


Figure 3. Crystallographic views of framework structures of (top) **1a** and (bottom) **3** along the *b* crystal axis (C, gray; O, red; Mn, cyan; Ni, green). The arrows propose how the chelating carboxylate groups coordinated to terminal Mn^{2+} ions (Mn2 and Mn2A) of the Mn_3 SBUs in **1a** adapt to connect the inserted Ni^{2+} (Ni1).

along the *b* axis. The 3D framework of **1a** can be viewed as discrete 2D layers interconnected by the carboxylate groups coordinated to the terminal Mn^{2+} cations (Mn2 and Mn2A) of the Mn_3 SBUs in a chelating coordination mode. The distance between neighboring layers is 11.664 Å. We hypothesize that the chelating carboxylate groups in **1a** are cleaved from the terminal Mn^{2+} cations and that two proximal (now unbound) carboxylate groups coordinate to an inserted Ni^{2+} cation (Ni1). These would be located at apical positions, with ligated solvent molecules occupying the equatorial plane of the resulting octahedral geometry. In addition, each terminal Mn^{2+} of the Mn_3 SBU (with 85% probability) in **1a** is displaced by a Ni^{2+} ion, with two aquo ligands replacing the cleaved chelating carboxylate group to maintain an octahedral geometry. The overall result of this process would be the trimetallic NiMnNi cluster as the SBU of **3**. It is noted that to accommodate the insertion of Ni^{2+} between the 2D layers of **1a**, these layers are pushed ~ 5 Å further apart in **3**, a feature directed by a conformational change in the L^4 linker. As a result, the *a* axis of **3** is significantly longer than that of **1a**, with an overall expansion of 33% upon SC–SC transformation. It is worth mentioning that attempts to synthesize **2** and **3** by conventional means (by combining mixed metal salts) failed, indicating that cation-insertion-induced SC–SC transformations represent a

feasible method for the generation of new coordination compounds from anionic MOFs constructed with flexible ligands.

Photometric experiments were conducted to establish the cation uptake capabilities and kinetics of bulk **1a** over a 48 h period (Figure S5). Co^{2+} was used as a suitable probe for uptake experiments because of its stability and UV spectroscopic profile. Framework **1a** was introduced into a 0.2 M DMF solution of cobalt(II) nitrate, and the concentration was measured as a function of time; the observed Co^{2+} concentration was found to decrease by 19% over 8.5 and 37% over 24 h. No significant decrease in Co^{2+} concentration was detected after 24 h, indicating uptake completion. The overall Co^{2+} uptake capacity of **1a** was found to be $3.12 \text{ mol mol}^{-1}$ (93 mg g^{-1}), which correlates with the results of SCXRD and EDX analysis. Additional EDX studies were performed to evaluate the selective uptake/exchange capabilities of **1a** toward a series of divalent metal ions ($Zn^{2+} > Cu^{2+} > Co^{2+} > Ni^{2+} \gg Mg^{2+} > Ca^{2+} > Sr^{2+}$). It was further demonstrated that crystals of **1a** selectively capture Cu^{2+} from a DMF solution containing equimolar amounts of Cu^{2+} and Ca^{2+} , implying that **1a** could be used to sequester divalent cations from a mixture (Table S1 in the SI). Interestingly, **1a** shows highly selective uptake of TM^{2+} ions in the presence of multiple competing alkali-metal cations such as Li^+ and Na^+ . Powder XRD (PXRD) and inductively coupled plasma optical emission spectroscopy (ICP-OES) studies of crystalline **1a** immersed in a DMF solution of either lithium or sodium nitrate showed that the anionic framework of **1a** remained unchanged but that the $NH_2(CH_3)_2^+$ counterions were fully replaced by Li^+ or Na^+ ions. Subsequent competition reactions between combinations of either cobalt(II) nitrate or nickel(II) nitrate and lithium nitrate or sodium nitrate followed by ICP-OES and EDX measurements indicated that either Co^{2+} or Ni^{2+} ions were preferentially sequestered by **1a**, with only trace amounts of Li^+ or Na^+ detected (Table S2). The soft framework of **1a** shows a strong preference for Co^{2+}/Ni^{2+} via SC–SC processes, and this may be explained by the significantly stronger interaction of carboxylate groups with the TM^{2+} cations.

The ability to interchange and control the metal composition in such systems has the clear potential to vary the magnetic properties of the resulting solid.⁴ Magnetic susceptibility measurements on powdered microcrystalline samples of complexes **1–3** were carried out in an applied field of 0.1 T, and the data are plotted as the $\chi_M T$ product versus temperature (Figure S6). For all of the compounds, the data are somewhat similar: $\chi_M T$ decreases slowly with decreasing temperature, indicative of relatively weak antiferromagnetic interactions between neighboring metal ions. The plots of χ^{-1} versus *T* (not shown) were linear, permitting fits to the Curie–Weiss law, $\chi^{-1} = (T - \Theta)/C$, which afforded Weiss constants (Θ) of -14.4 K (**1a**), -10.5 K (**2**), and -9.30 K (**3**). For complex **1**, the susceptibility data could be fitted to the simple isotropic Hamiltonian $\hat{H} = -2J(\hat{S}_{Mn1} \cdot \hat{S}_{Mn2} + \hat{S}_{Mn2} \cdot \hat{S}_{Mn3})$, which describes the system as a series of magnetically isolated $Mn1-Mn2-Mn3$ linear trimers in which all of the $M \cdots M$ interactions are equivalent. The upper solid red line in Figure S6 is the fit with $J_{Mn-Mn} = -1.42 \text{ cm}^{-1}$ and $g = 2.00$. The data for complex **3** could be treated in a similar fashion by assuming isolated linear $Ni1-Mn1-Ni2$ chains [$\hat{H} = -2J(\hat{S}_{Ni1} \cdot \hat{S}_{Mn1} + \hat{S}_{Mn1} \cdot \hat{S}_{Ni2})$] and noninteracting (paramagnetic) Ni monomers. The lower solid red line in Figure S6 is the fit with $J_{Ni-Mn} = -1.43 \text{ cm}^{-1}$ and $g = 2.21$. The magnetochemical analysis of $Co(II)$ -based complexes

is nontrivial because of the combined effects of spin–orbit coupling and the distortion of the octahedral crystal field. This and the presence of significant crystallographic disorder precluded any meaningful quantitative analysis of the magnetic data for complex 2.

In summary, we have demonstrated that soft anionic MOFs (**1a** and **1b**) are capable of sequestering metal cations through cooperative SC–SC processes, resulting in novel neutral and heterobimetallic systems with rearranged framework structures. These SC–SC transformations are directed by adaptation of the conformation and coordination modes of the flexible organic carboxylate linker (L^{4-}) to meet the coordination environment of inserted/exchanged metal ions, a process involving cooperative breakage/formation of metal–carboxylate coordination bonds in the solid state. These anionic MOFs also exhibit exceptional uptake/exchange selectivity for TM^{2+} ions in the presence of competing alkali-metal cations. In stark contrast to the rigid open 3D frameworks of zeolites, which tend to be less affected by ion exchange, the framework flexibility observed for the soft anionic MOFs reported here holds great potential for the design of selective sensors, selective ion-exchange media, and materials for the removal of toxic heavy-metal ions, all of which will be the focus of future studies.²⁰

■ ASSOCIATED CONTENT

Supporting Information

Sample preparation and characterization, including TGA, PXRD, and EDX data; crystallographic data (CIF); and additional structural figures. This material is available free of charge via the Internet at <http://pubs.acs.org>.

■ AUTHOR INFORMATION

Corresponding Author

S.J.Dalgarno@hw.ac.uk; praveen.thallapally@pnnl.gov

Notes

The authors declare no competing financial interest.

■ ACKNOWLEDGMENTS

This work was supported by the EPSRC, the Laboratory Direct Research, and the U.S. Department of Energy, Office of Basic Energy Sciences, Division of Materials Sciences and Engineering (Award KC020105-FWP12152). Pacific Northwest National Laboratory is operated by Battelle for the U.S. Department of Energy under Contract DE-AC05-76RL01830.

■ REFERENCES

- (1) For recent reviews, see: (a) Rowsell, J. L. C.; Yaghi, O. M. *Angew. Chem., Int. Ed.* **2005**, *44*, 4670. (b) Ma, S.; Zhou, H.-C. *Chem. Commun.* **2010**, *46*, 44. (c) Sumida, K.; Rogow, D. L.; Mason, J. A.; McDonald, T. M.; Bloch, E. D.; Herm, Z. R.; Bae, T.-H.; Long, J. R. *Chem. Rev.* **2012**, *112*, 724. (d) Liu, J.; Thallapally, P. K.; McGrail, B. P.; Brown, D. R.; Liu, J. *Chem. Soc. Rev.* **2012**, *41*, 2308.
- (2) Li, J.-R.; Sculley, J.; Zhou, H.-C. *Chem. Rev.* **2012**, *112*, 869.
- (3) (a) Min, K. S.; Suh, M. P. *J. Am. Chem. Soc.* **2000**, *122*, 6834. (b) Fei, H.; Rogow, D. L.; Oliver, S. R. *J. Am. Chem. Soc.* **2010**, *132*, 7202.
- (4) Kurmoo, M. *Chem. Soc. Rev.* **2009**, *38*, 1353.
- (5) (a) Lee, J. Y.; Farha, O. K.; Roberts, J.; Scheidt, K. A.; Nguyen, S. T.; Hupp, J. T. *Chem. Soc. Rev.* **2009**, *38*, 1450. (b) Ma, L.; Abney, C.; Lin, W. *Chem. Soc. Rev.* **2009**, *38*, 1248.
- (6) Wang, C.; Zhang, T.; Lin, W. *Chem. Rev.* **2012**, *112*, 1084.
- (7) For recent reviews, see: (a) Uemura, K.; Matsuda, R.; Kitagawa, S. *J. Solid State Chem.* **2005**, *178*, 2420. (b) Fletcher, A. J.; Thomas, K.

M.; Rosseinsky, M. J. *J. Solid State Chem.* **2005**, *178*, 2491. (c) Bradshaw, D.; Claridge, J. B.; Cussen, E. J.; Prior, T. J.; Rosseinsky, M. J. *Acc. Chem. Res.* **2005**, *38*, 273. (d) Kitagawa, S. *Nat. Chem.* **2009**, *1*, 695.

(8) For example, see: (a) Biradha, K.; Fujita, M. *Angew. Chem., Int. Ed.* **2002**, *41*, 3392. (b) Pretsch, T.; Chapman, K. W.; Halder, G. J.; Kepert, C. J. *Chem. Commun.* **2006**, 1857. (c) Liu, D.; Ren, Z.-G.; Li, H.-X.; Lang, J.-P.; Li, N.-Y.; Abrahams, B. F. *Angew. Chem., Int. Ed.* **2010**, *49*, 4767. (d) Sun, J.; Dai, F.; Yuan, W.; Bi, W.; Zhao, X.; Sun, W.; Sun, D. *Angew. Chem., Int. Ed.* **2011**, *50*, 7061. (e) Falkowski, J. M.; Wang, C.; Liu, S.; Lin, W. *Angew. Chem., Int. Ed.* **2011**, *50*, 8674.

(9) (a) Cussen, E. J.; Claridge, J. B.; Rosseinsky, M. J.; Kepert, C. J. *J. Am. Chem. Soc.* **2002**, *124*, 9574. (b) Biradha, K.; Fujita, M. *J. Am. Chem. Soc.* **2004**, *126*, 14063. (c) Dybtsev, D. N.; Chun, H.; Kim, K. *Angew. Chem., Int. Ed.* **2004**, *43*, 5033. (d) Bourrelly, S.; Llewellyn, P. L.; Serre, C.; Millange, F.; Loiseau, T.; Férey, G. *J. Am. Chem. Soc.* **2005**, *127*, 13519.

(10) (a) Zhang, J. P.; Chen, X. M. *J. Am. Chem. Soc.* **2008**, *130*, 6010. (b) Shimomura, S.; Higuchi, M.; Matsuda, R.; Yoneda, K.; Hijikata, Y.; Kubota, Y.; Mita, Y.; Kim, J.; Takata, M.; Kitagawa, S. *Nat. Chem.* **2010**, *2*, 633. (c) Yanai, N.; Kitayama, K.; Hijikata, Y.; Sato, H.; Matsuda, R.; Kubota, Y.; Takata, M.; Mizuno, M.; Uemura, T.; Kitagawa, S. *Nat. Mater.* **2011**, *10*, 787. (d) Seo, J.; Bonneau, C.; Matsuda, R.; Takata, M.; Kitagawa, S. *J. Am. Chem. Soc.* **2011**, *133*, 9005. (e) Park, J.; Yuan, D.; Pham, K. T.; Li, J.-R.; Yakovenko, A.; Zhou, H.-C. *J. Am. Chem. Soc.* **2012**, *134*, 99.

(11) (a) Cheng, X. N.; Zhang, W. X.; Chen, X. M. *J. Am. Chem. Soc.* **2007**, *129*, 15738. (b) Kaneko, W.; Ohba, M.; Kitagawa, S. *J. Am. Chem. Soc.* **2007**, *129*, 13706.

(12) (a) Chu, Q. L.; Swenson, D. C.; MacGillivray, L. R. *Angew. Chem., Int. Ed.* **2005**, *44*, 3569. (b) Medishetty, R.; Koh, L. L.; Kole, G. K.; Vittal, J. J. *Angew. Chem., Int. Ed.* **2011**, *50*, 10949.

(13) (a) Mellot-Draznieks, C.; Serre, C.; Surble, S.; Férey, G. *J. Am. Chem. Soc.* **2005**, *127*, 16273. (b) Serre, C.; Mellot-Draznieks, C.; Surble, S.; Audebrand, N.; Filinchuk, Y.; Férey, G. *Science* **2007**, *315*, 1828. (c) Willans, C. E.; French, S.; Anderson, K. M.; Barbour, L. J.; Gertenbach, J.-A.; Lloyd, G. O.; Dyer, R. J.; Steed, J. W. *Dalton Trans.* **2011**, *40*, 573.

(14) Maji, T. K.; Matsuda, R.; Kitagawa, S. *Nat. Mater.* **2007**, *6*, 142. (15) (a) Das, S.; Kim, H.; Kim, K. *J. Am. Chem. Soc.* **2009**, *131*, 3814. (b) Plabst, M.; McCusker, L. B.; Bein, T. *J. Am. Chem. Soc.* **2009**, *131*, 18112.

(16) (a) Serre, C.; Millange, F.; Thouvenot, C.; Nogues, M.; Marsolier, G.; Loueër, D.; Férey, G. *J. Am. Chem. Soc.* **2002**, *124*, 13519. (b) Loiseau, T.; Serre, C.; Huguenard, C.; Fink, G.; Taulelle, F.; Henry, M.; Bataille, T.; Férey, G. *Chem.—Eur. J.* **2004**, *10*, 1373.

(17) (a) Kim, H.; Suh, M. P. *Inorg. Chem.* **2005**, *44*, 810. (b) Thallapally, P. K.; Tian, J.; Kishan, M. R.; Fernandez, C. A.; Dalgarno, S. J.; McGrail, P. B.; Warren, J. E.; Atwood, J. L. *J. Am. Chem. Soc.* **2008**, *130*, 16842. (c) Tian, J.; Motkuri, R. K.; Thallapally, P. K. *Cryst. Growth Des.* **2010**, *10*, 3843.

(18) (a) Guo, Z.-G.; Cao, R.; Wang, X.; Li, H.; Yuan, W.; Wang, G.; Wu, H.; Li, J. *J. Am. Chem. Soc.* **2009**, *131*, 6894. (b) Kishan, M. R.; Tian, J.; Thallapally, P. K.; Fernandez, C. A.; Dalgarno, S. J.; Warren, J. E.; McGrail, B. P.; Atwood, J. L. *Chem. Commun.* **2010**, *46*, 538. (c) Liu, T.-F.; Lü, J.; Guo, Z.-G.; Proserpio, D. M.; Cao, R. *Cryst. Growth Des.* **2010**, *10*, 1489. (d) Liu, T.-F.; Lü, J.; Lin, X.; Cao, R. *Chem. Commun.* **2010**, *46*, 8439. (e) Liang, L.-L.; Ren, S.-B.; Zhang, J.; Li, Y.-Z.; Du, H.-B.; You, X.-Z. *Dalton Trans.* **2010**, *39*, 7723.

(19) Liu, T.-F.; Lü, J.; Tian, C.; Cao, M.; Lin, Z.; Cao, R. *Inorg. Chem.* **2011**, *50*, 2264.

(20) Kreno, L. E.; Leong, K.; Farha, O. M.; Allendorf, M.; Van Duyne, R. P.; Hupp, J. T. *Chem. Rev.* **2012**, *112*, 1105.